Meccanica (2007) 42: 547–553
DOI 10.1007/s11012-007-9079-1

Dynamic instability of axially loaded shafts in the Mathieu map

Francesco A. Raffa · Furio Vatta

Received: 15 March 2007 / Accepted: 7 June 2007 / Published online: 4 August 2007

Abstract It is shown that the Mathieu eigenvalues can be straightforwardly utilized to study the instability regions of an axially loaded simply supported shaft, the shaft being modeled as a continuous rotating beam. When a harmonic axial load is taken into account, the equation of motion of the system, here written according to the Lagrangian formulation of continuous systems, proves to be the Mathieu equation. It follows that the conditions for the stable or unstable motion of the shaft can be graphically investigated once the operation line corresponding to an actual rotating shaft is drawn in the Mathieu map.

Keywords Continuous beams · Mathieu's equation · Dynamic stability · Rotordynamics · Mechanics of machines

Abbreviations

A, l	Area, length
E, G	Young's modulus, shear modulus
ρ	Mass density
χ	Shear factor
J	Diametral area moment of inertia
J_m, I_m	Diametral, polar mass moment of inertia per unit length
N_s, N_d	Amplitude of the axial load static, dynamic component
$\mathcal{T}$	Kinetic energy density
$\mathcal{V}$	Potential energy density
$\mathcal{W}$	Work density
$\mathcal{L}$	Lagrangian density
x, y, s	Fixed coordinates
t	Time
u, v	Displacements in the x, y axes
ϑ_x, ϑ_y	Bending rotations about the x, y axes
w	Complex displacement
λ_k, Λ_k	k-th natural frequencies
ω, Ω	Rotational speed, axial excitation frequency

F.A. Raffa (✉) · F. Vatta
Dipartimento di Meccanica, Politecnico di Torino, Corso Duca degli Abruzzi 24, 10129 Torino, Italy
e-mail: francesco.raffa@polito.it

1 Introduction

This work deals with the problem of the instability of a simply supported continuous shaft subjected to an axial load $N(t) = N_s + N_d \cos \Omega t$, which is known to be the source of a potentially unstable behavior of the shaft, and shows that a graphical solution can be readily obtained once the governing equation of the problem is recognized to be the canonical Mathieu equation. The shaft, depicted in Fig. 1, is assumed to be a continuous beam modeled according to: I—the Bernoulli–Euler theory with the further consideration of the shear effect and II—the rotating Rayleigh beam theory, which adds both the rotary inertia and the gyroscopic effect of the beam to the translational inertia

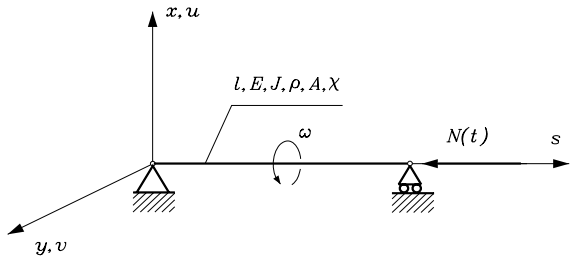

Fig. 1 A rotating shaft subjected to the static plus time harmonic axial load $N(t) = N_s + N_d \cos \Omega t$

of the Bernoulli–Euler beam. It is assumed that the lateral displacements of the beam are so small that axial motions are negligible; from a dynamical point of view this means that the axial excitation frequency does not induce axial resonance.

Within this physical framework, the formalism of the Lagrangian formulation of continuous systems is applied to obtain the Lagrangian equations of motion, which are then grouped into a single governing equation with respect to $w = u + iv$. Such equation turns out to be the Mathieu equation in its canonical form. This circumstance leads quite naturally to a neat graphical method to investigate the stability of the rotating shaft: in the Mathieu map the stability regions are identified analyzing the intersections between the branches of the Mathieu eigenvalues, which are reported in literature, and the straight operation line of the shaft. In particular, one can readily establish the ranges of values of the physical parameters, which prevent the shaft from crossing unstability regions.

Notice that, while this benchmark problem of rotordynamics has been largely investigated (see for example [1] where, however, the Mathieu equation is not mentioned), the graphical approach presented in this paper is original, to the best of the authors' knowledge. In fact, the Mathieu equation theory in rotordynamics has been so far utilized resorting to the explicit construction of the boundaries between stable and unstable regions [2, 3], whose application to rotor systems is described, e.g., in [4], where a discrete cantilever shaft-disk system is analyzed, while here it is shown that the stable and unstable regions of a rotating shaft can be identified applying a straightforward procedure which entails the use of the problem-independent Mathieu eigenvalues.

The authors are fully aware that their approach has been successfully utilized in other fields and mention in this regard the representative investigation reported in [5], where the conditions for the stable motion of ions in a quadrupole field are thoroughly examined.

2 Equations of motion

The following procedure is applied: for both shaft models the kinetic and potential energy densities are obtained as a particular case of the variational formulation reported in [6], where the complete beam model, usually referred to as the continuous rotating Timoshenko shaft, is considered. To the external axial load, which is not derivable from a potential function, one associates the work density [7]

$$\mathcal{W} = \frac{1}{2} N \left[\left(\frac{\partial u}{\partial s} \right)^2 + \left(\frac{\partial v}{\partial s} \right)^2 \right]. \tag{1}$$

For a continuous one-dimensional system it is well-known that the Lagrangian equations of motion follow from the Hamilton principle, i.e.,

$$\delta \int_{t_1}^{t_2} \int_0^l (\mathcal{T} - \mathcal{V} + \mathcal{W})\, ds\, dt = 0.$$

Upon defining $\mathcal{L} = \mathcal{T} - \mathcal{V} + \mathcal{W}$ and with $\mathcal{L}$ depending, for the sake of generality, on the continuous variables (fields), here denoted as φ_a's, as well as on their first and second derivatives, such equations can be given the compact form

$$\frac{\partial \mathcal{L}}{\partial \varphi_a} - \partial_\mu \left(\frac{\partial \mathcal{L}}{\partial \partial_\mu \varphi_a} \right) + \partial_\mu \partial_\nu \left(\frac{\partial \mathcal{L}}{\partial \partial_\mu \partial_\nu \varphi_a} \right) = 0, \quad a = 1, 2, \ldots. \tag{2}$$

For convenience, in (2) the implicit summation convention is adopted, with $\mu, \nu = 0, 1$ repeated indexes, while for the first derivatives $\partial_0 \equiv \partial/\partial t$, $\partial_1 \equiv \partial/\partial s$, this convention being extended to the second derivatives, e.g., $\partial^2_{01} \varphi_a \equiv \partial^2 \varphi_a / \partial s \partial t$.

I Bernoulli-Euler model plus shear effect

The kinetic and potential energy densities read

$$\mathcal{T} = \frac{1}{2} \rho A \left[\left(\frac{\partial u}{\partial t} \right)^2 + \left(\frac{\partial v}{\partial t} \right)^2 \right], \tag{3}$$

$$\mathcal{V} = \frac{1}{2} EJ \left[\left(-\frac{\partial^2 v}{\partial s^2} \right)^2 + \left(\frac{\partial^2 u}{\partial s^2} \right)^2 \right] + \frac{1}{2} \frac{GA}{\chi} \left[\left(\frac{\partial v}{\partial s} + \vartheta_x \right)^2 + \left(\frac{\partial u}{\partial s} - \vartheta_y \right)^2 \right]. \tag{4}$$

With the φ_a's, $a = 1, \ldots, 4$, identified as the fields u, v, ϑ_x, ϑ_y and $\partial\mathcal{L}/\partial\partial_\mu\partial_\nu\varphi_a = 0$, as $\mathcal{L}$ does not contain the second derivatives of the φ_a's, the four Lagrangian equations of motion, obtained from (2), prove to be coupled with respect to either u and ϑ_y or v and ϑ_x. Uncoupling leads to the equation of motion with respect to w

$$EJ\frac{\partial^4 w}{\partial s^4} - \chi\rho J\frac{E}{G}\frac{\partial^4 w}{\partial s^2\partial t^2} + \rho A\frac{\partial^2 w}{\partial t^2} + N\frac{\partial^2 w}{\partial s^2} = 0. \tag{5}$$

It is well-known that this model does not include any effect related to the rotation of the shaft. Disregarding the shear deformation term in (5) leads to the equation of motion of the Bernoulli–Euler beam.

II Rayleigh model
For this model one has

$$\begin{aligned}\mathcal{T} = {} & \frac{1}{2}\rho A\left[\left(\frac{\partial u}{\partial t}\right)^2 + \left(\frac{\partial v}{\partial t}\right)^2\right] \\ & + \frac{1}{2}J_m\left[\left(-\frac{\partial^2 v}{\partial s\partial t}\right)^2 + \left(\frac{\partial^2 u}{\partial s\partial t}\right)^2\right] \\ & + \frac{1}{2}I_m\omega\left(-\frac{\partial u}{\partial s}\frac{\partial^2 v}{\partial s\partial t} + \frac{\partial v}{\partial s}\frac{\partial^2 u}{\partial s\partial t}\right),\end{aligned} \tag{6}$$

$$\mathcal{V} = \frac{1}{2}EJ\left[\left(-\frac{\partial^2 v}{\partial s^2}\right)^2 + \left(\frac{\partial^2 u}{\partial s^2}\right)^2\right]. \tag{7}$$

With φ_1, φ_2 corresponding to the fields u, v and $\partial\mathcal{L}/\partial\varphi_a = 0$, as $\mathcal{L}$ does not depend explicitly on either of the φ_a's, the two Lagrangian equations derived from (2) prove to be coupled with respect to u and v; in terms of w one finds

$$\begin{aligned}EJ\frac{\partial^4 w}{\partial s^4} - J_m\frac{\partial^4 w}{\partial s^2\partial t^2} + \rho A\frac{\partial^2 w}{\partial t^2} + iI_m\omega\frac{\partial^3 w}{\partial s^2\partial t} \\ + N\frac{\partial^2 w}{\partial s^2} = 0.\end{aligned} \tag{8}$$

Here the equation of motion of the Bernoulli–Euler beam is obtained neglecting in (8) the two terms associated to the rotary inertia and the gyroscopic effect of the shaft.

3 Simply supported shaft

For the simply supported continuous shaft one substitutes w in both (5) and (8) with the well-known solution which satisfies the boundary conditions at the supports

$$w(s,t) = f_k(t)\sin\frac{k\pi s}{l}, \quad k = 1, 2, \ldots, \tag{9}$$

and obtains the following results.

I Bernoulli–Euler model plus shear effect
The equation in f_k

$$\begin{aligned}&\left[\rho A + \chi\rho J\frac{E}{G}\left(\frac{k\pi}{l}\right)^2\right]\frac{d^2 f_k}{dt^2} \\ &\quad + \left(\frac{k\pi}{l}\right)^2\left[EJ\left(\frac{k\pi}{l}\right)^2 - N\right]f_k = 0,\end{aligned} \tag{10}$$

can be written in dimensionless parameters setting $\Omega t = 2z$

$$\frac{d^2 f_k}{dz^2} + \left(\frac{2\lambda_k}{\Omega}\right)^2\left[\left(1 - \frac{N_s}{N_{c,k}}\right) - \frac{N_d}{N_{c,k}}\cos 2z\right]f_k = 0, \tag{11}$$

where λ_k and $N_{c,k}$ are the k-th natural frequency of the Bernoulli–Euler beam including the shear deformation effect and the k-th Euler critical load of the simply supported beam, respectively,

$$\lambda_k = \frac{(\frac{k\pi}{l})^2\sqrt{\frac{EJ}{\rho A}}}{\sqrt{1 + \chi\frac{N_{c,k}}{GA}}}, \tag{12}$$

$$N_{c,k} = \left(\frac{k\pi}{l}\right)^2 EJ. \tag{13}$$

For the k-th mode of the shaft (11) is readily recognized to be the Mathieu differential equation in its canonical form [8]

$$\frac{d^2 y}{dz^2} + (a - 2q\cos 2z)y = 0, \tag{14}$$

where a and $y(z)$ are the Mathieu eigenvalues and eigenfunctions. It is well-known that there exist two families of independent Mathieu's eigenfunctions of integral order, the cosine-elliptic and sine-elliptic, $ce_m(z,q), m = 0, 1, 2, \ldots$ and $se_m(z,q), m = 1, 2, 3, \ldots$, where m is the order. The Mathieu eigenvalues associated to ce_m and se_m, usually denoted as $a_m(q)$ and $b_m(q)$, respectively, are given as power series of

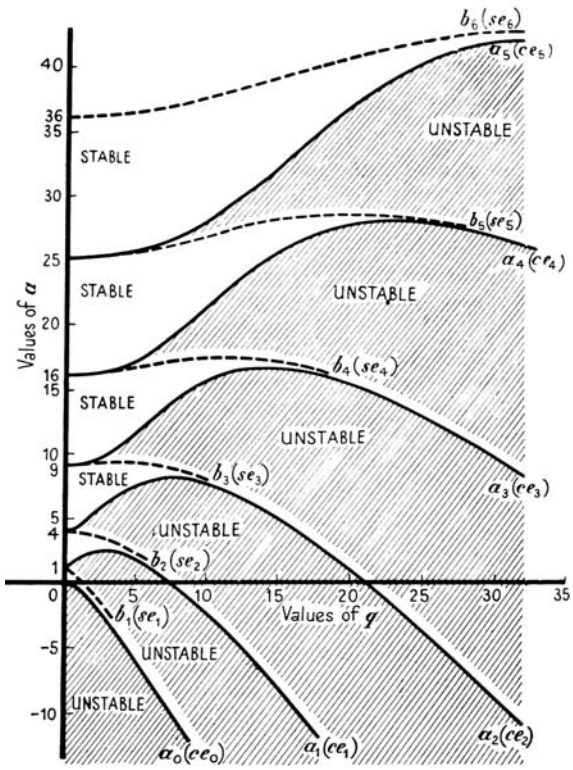

Fig. 2 Eigenvalues of Mathieu's equation (graph taken from [8], p. 40)

q, as reported, e.g., in [8]. Figure 2 illustrates the variation of the Mathieu eigenvalues as functions of q.

For a given k the correspondence between our example, (11), and the general case, (14), is

$$y \equiv f_k, \tag{15}$$

$$a \equiv \left(\frac{2\lambda_k}{\Omega}\right)^2 \left(1 - \frac{N_s}{N_{c,k}}\right), \tag{16}$$

$$q \equiv \left(\frac{\sqrt{2}\lambda_k}{\Omega}\right)^2 \frac{N_d}{N_{c,k}}. \tag{17}$$

In the Mathieu map (a, q) (16) and (17) define the straight line representing the operation line of the actual physical problem. Its slope is

$$S_I = 2\frac{1 - \frac{N_s}{N_{c,k}}}{\frac{N_d}{N_{c,k}}}. \tag{18}$$

II Rayleigh model

The equation in $f_k(t)$ proves to be

$$\left[\rho A + J_m\left(\frac{k\pi}{l}\right)^2\right]\frac{d^2 f_k}{dt^2} - i I_m \omega \left(\frac{k\pi}{l}\right)^2 \frac{df_k}{dt} + \left(\frac{k\pi}{l}\right)^2 \left[EJ\left(\frac{k\pi}{l}\right)^2 - N\right] f_k = 0. \tag{19}$$

According to the standard transformation technique [9], the first derivative term in (19) is removed defining the new dependent variable $g_k(t)$,

$$f_k(t) = g_k(t) \exp\left[\frac{1}{2}\frac{i I_m \omega (k\pi/l)^2}{\rho A + J_m (k\pi/l)^2} t\right],$$

where the harmonic exponential term does not influence the stability conditions of the shaft.

Letting again $\Omega t = 2z$, (19) becomes

$$\frac{d^2 g_k}{dz^2} + \left(\frac{2\Lambda_k}{\Omega}\right)^2 \left[\left(1 - \frac{N_s}{N_{c,k}} + \gamma_k \omega^2\right) - \frac{N_d}{N_{c,k}} \cos 2z\right] g_k = 0. \tag{20}$$

In (20) Λ_k is the k-th natural frequency of the vibrating Rayleigh beam

$$\Lambda_k = \frac{(\frac{k\pi}{l})^2 \sqrt{\frac{EJ}{\rho A}}}{\sqrt{1 + \frac{J_m}{\rho A}(\frac{k\pi}{l})^2}}, \tag{21}$$

while in the term corresponding to the rotation of the shaft one sets

$$\gamma_k = \frac{\rho J}{EA + N_{c,k}}. \tag{22}$$

For each fixed k (20) is a further example of the Mathieu differential equation in its canonical form (14). The correspondence between our example and the general case is

$$a \equiv \left(\frac{2\Lambda_k}{\Omega}\right)^2 \left(1 - \frac{N_s}{N_{c,k}} + \gamma_k \omega^2\right), \tag{23}$$

$$q \equiv \left(\frac{\sqrt{2}\Lambda_k}{\Omega}\right)^2 \frac{N_d}{N_{c,k}}, \tag{24}$$

the slope of the operation line in the Mathieu map being now

$$S_{II} = 2\frac{1 - \frac{N_s}{N_{c,k}} + \gamma_k \omega^2}{\frac{N_d}{N_{c,k}}}. \tag{25}$$

4 Results and discussion

In principle, one can readily evaluate the effect of all the parameters appearing in the previous mathematical treatment. Equations (16–18) and (23–25) make clear that for both models increasing N_s and N_d gives a smaller slope of the operation line, while, as Ω increases, the operating point, i.e., the point on the operation line corresponding to the given shaft configuration, moves along the line toward the origin of the Mathieu map (a, q). Notice also that the higher the mode order k, the larger the slope of the operation line for both models.

As for the parameters characterizing a specific model, in the Bernoulli–Euler beam including the shear deformation effect, higher values of χ make the operating point move toward the origin of the Mathieu map; in this model, manifestly, the variation of the shear factor can be considered rather unphysical for a rotating shaft, while for a vibrating shaft a wide range of cross sections with different values of χ can be actually utilized. In the Rayleigh model, increasing ω results in a larger slope of the operation line, while increasing the rotary inertia makes the operating point move toward the origin of the Mathieu map.

Notice that the net result of modifying the above parameters can be a stable or unstable condition of the shaft depending on the initial position of the operating point on the operation line.

To verify the above considerations an instability analysis has been carried out with reference to the first mode of vibration of a simply supported shaft, whose relevant data are the same as in [4]: $l = 0.5$ m, $A = 314 \times 10^{-6}$ m^2, $\chi = 1.124$, $\rho = 7860$ kg/m^3, $E = 2.07 \times 10^{11}$ Pa, $G = 7.96 \times 10^{10}$ Pa.

The numerical results show that the operation lines and the operating points of this shaft are not appreciably influenced by the values of χ and ω. Here, therefore, the results are given only for the Bernoulli–Euler model and the attention is focused on the parameters

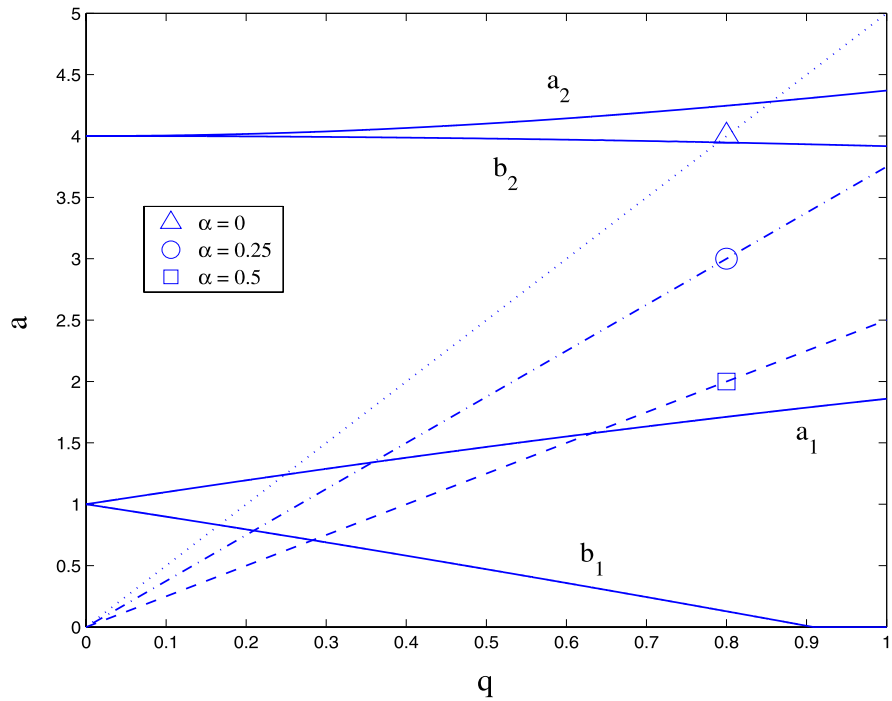

Fig. 3 Effect of the static load component on the stability of the simply supported shaft subjected to axial load ($\alpha = 0, 0.25, 0.5$; $\beta = 0.4$, $\Gamma = 1$)

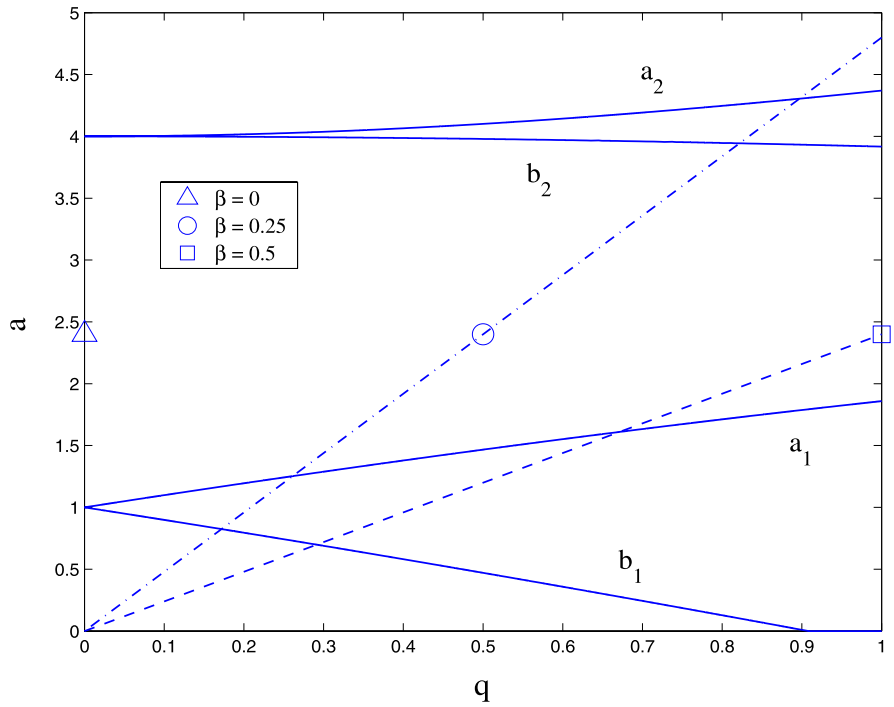

Fig. 4 Effect of the dynamic load component on the stability of the simply supported shaft subjected to axial load ($\beta = 0, 0.25, 0.5$; $\alpha = 0.4$, $\Gamma = 1$)

Ω, N_s, N_d, which are physically associated to the external excitation. To simplify the notation one defines the following dimensionless variables

$$\alpha = \frac{N_s}{N_{c,1}}, \qquad \beta = \frac{N_d}{N_{c,1}}, \qquad \Gamma = \Omega\sqrt{\frac{\rho A}{EJ}}\left(\frac{l}{\pi}\right)^2, \tag{26}$$

where α and β can be named static and dynamic load factor, respectively, while Γ is the dimensionless frequency of the axial load; $N_{c,1}$ is the fundamental Euler critical load from (13) with $k = 1$.

The influence of α, β and Γ on the stability of the shaft can be realized from the Mathieu maps reported in Figs. 3, 4 and 5, where the solid lines refer to the Mathieu eigenvalues a_1, b_1, a_2, b_2 and the discontinuous lines are the operation lines of the shaft. Specifically, in Fig. 3 the operation lines and the operating points are reported for different values of the static load factor ($\alpha = 0, 0.25, 0.5$), with $\beta = 0.4$, $\Gamma = 1$, while the effect of the dynamic axial load component is shown in Fig. 4 where $\beta = 0, 0.25, 0.5$, with $\alpha = 0.4$, $\Gamma = 1$. Finally, in Fig. 5 the shift of the operating point along the operation line induced by the variation of the axial frequency is reported for $\Gamma = 0.8, 1.6, 2.4, 3.2$ with $\alpha = \beta = 0.25$.

5 Conclusions

In this paper the problem of a continuous axially loaded shaft has been considered. For the simply supported case the governing equations of motion, derived applying the Lagrangian formulation of continuous systems to both the Bernoulli–Euler beam with shear deformation effect and the Rayleigh rotating beam, prove to reduce to the Mathieu equation.

This circumstance has been exploited to investigate the dynamic instability of the shaft in quite a direct way: the boundaries of the stable and unstable regions are in fact clearly assessed analyzing the intersections between the operation line of the shaft and the branches of the Mathieu eigenvalues in the Mathieu map (a, q). In particular, this graphical approach has been utilized to evaluate the influence of the parameters related to the axial load (static and dynamic load

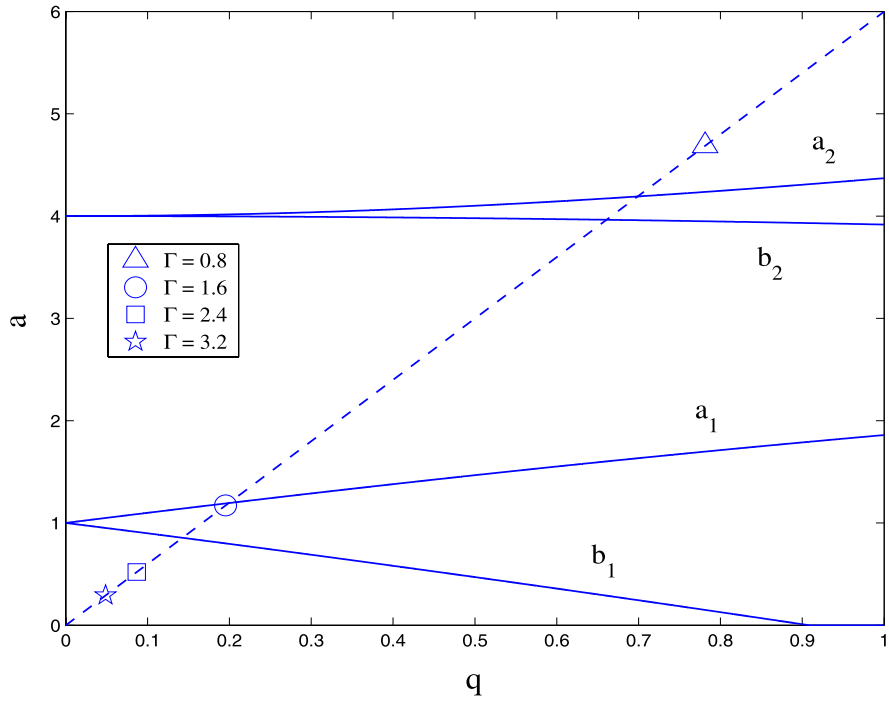

Fig. 5 Effect of the excitation frequency on the stability of the simply supported shaft subjected to axial load ($\Gamma = 0.8, 1.6, 2.4, 3.2$; $\alpha = \beta = 0.25$)

components, frequency of excitation) on the behavior of the shaft.

From a theoretical point of view, one should mention that the proposed method does not apply to the rotating Timoshenko beam and to other boundary conditions that may be of some interest (as clamped-clamped and clamped-free ends). Indeed the equations of motion in these cases do not reduce to the Mathieu equation, so that a finite element approach is commonly employed, as reported for example in [10].

References

1. Dimentberg FM (1961) Flexural vibrations of rotating shafts. Butterworth, London
2. Bolotin VV (1964) The dynamic stability of elastic systems. Holden-Day, San Francisco
3. Xie WC (2006) Dynamic stability of structures. Cambridge University Press, New York
4. Sheu HC, Chen LW (2000) A lumped mass model for parametric instability analysis of cantilever shaft-disk systems. J Sound Vib 234:331–348
5. Paul W (1990) Electromagnetic traps for charged and neutral particles. Rev Mod Phys 62:531–540
6. Raffa FA, Vatta F (1999) Gyroscopic effects analysis in the Lagrangian formulation of rotating beams. Meccanica 34:357–366
7. Meirovitch L (1967) Analytical methods in vibrations. Macmillan, New York
8. McLachlan NW (1964) Theory and application of Mathieu functions. Dover, New York
9. Cunningham WJ (1958) Introduction to nonlinear analysis. McGraw–Hill, New York
10. Chen LW, Ku DM (1992) Dynamic stability of a cantilever shaft-disk system. ASME J Vib Acoust 114:326–329